



Elementary Structural Motifs in a Random Network of Cytosine Adsorbed on a Gold(111) Surface

Roberto Otero *et al.*

Science **319**, 312 (2008);

DOI: 10.1126/science.1150532

This copy is for your personal, non-commercial use only.

If you wish to distribute this article to others, you can order high-quality copies for your colleagues, clients, or customers by [clicking here](#).

Permission to republish or repurpose articles or portions of articles can be obtained by following the guidelines [here](#).

The following resources related to this article are available online at www.sciencemag.org (this information is current as of October 3, 2013):

Updated information and services, including high-resolution figures, can be found in the online version of this article at:

<http://www.sciencemag.org/content/319/5861/312.full.html>

Supporting Online Material can be found at:

<http://www.sciencemag.org/content/suppl/2008/01/22/1150532.DC1.html>

This article **cites 15 articles**, 2 of which can be accessed free:

<http://www.sciencemag.org/content/319/5861/312.full.html#ref-list-1>

This article has been **cited by** 34 article(s) on the ISI Web of Science

This article has been **cited by** 2 articles hosted by HighWire Press; see:

<http://www.sciencemag.org/content/319/5861/312.full.html#related-urls>

This article appears in the following **subject collections**:

Chemistry

<http://www.sciencemag.org/cgi/collection/chemistry>

7. G. Tenorio-Tagle, *Astron. Astrophys.* **71**, 59 (1979).
8. W. J. Henney, S. J. Arthur, M. T. García-Díaz, *Astrophys. J.* **627**, 813 (2005).
9. R. Subrahmanyam, W. M. Goss, D. F. Malin, *Astron. J.* **121**, 399 (2001).
10. W. H.-M. Ku, G. Chanan, *Astrophys. J.* **234**, L59 (1979).
11. M. R. Gagné, J.-P. Caillaud, J. R. Stauffer, *Astrophys. J.* **445**, 280 (1995).
12. E. D. Feigelson *et al.*, *Astrophys. J. Suppl. Ser.* **160**, 379 (2005).
13. F. Jansen *et al.*, *Astron. Astrophys.* **365**, L1 (2001).
14. L. Strüder *et al.*, *Astron. Astrophys.* **365**, L18 (2001).
15. M. J. L. Turner *et al.*, *Astron. Astrophys.* **365**, L27 (2001).
16. Materials and methods are available as supporting material on Science Online.
17. L. K. Townsley *et al.*, *Astrophys. J.* **593**, 874 (2003).
18. C. R. O'Dell, T. Doi, *Astron. J.* **125**, 277 (2003).
19. F. Palla, S. W. Stahler, *Astrophys. J.* **525**, 772 (1999).
20. L. K. Townsley *et al.*, *Astron. J.* **131**, 2140 (2006).
21. C. Leitherer, *Astrophys. J.* **326**, 356 (1988).
22. J. Castor, R. McCray, R. Weaver, *Astrophys. J.* **200**, L107 (1975).
23. D. N. Burrows, K. P. Singh, J. A. Nousek, G. P. Garmire, J. A. Good, *Astrophys. J.* **406**, 97 (1993).
24. A. Blaauw, in *The Physics of Star Formation and Early Evolution*, C. J. Lada, N. Kylafis, Eds. (Kluwer, Dordrecht, Netherlands, 1991), vol. C342, pp. 125–154.
25. R. Diehl, *N. Astron. Rev.* **46**, 547 (2002).
26. We thank D. Malin for providing the optical image of the Orion Nebula taken with the UK Schmidt telescope and granting permission to use it and R. Subrahmanyam and the American Astronomical Society for granting permission to reproduce the radio panel in Fig. 4D. This

research is based on observations obtained with XMM-Newton, a European Space Agency (ESA) science mission with instruments and contributions directly funded by ESA member states and the United States (NASA). M.A. acknowledges support from a Swiss National Science Foundation Professorship (PP002-110504), and S.S. from NASA grant NNG05GE69G.

Supporting Online Material

www.sciencemag.org/cgi/content/full/1149926/DC1
Materials and Methods
Figs. S1 to S3
Table S1

30 August 2007; accepted 15 November 2007
Published online 29 November 2007;
10.1126/science.1149926
Include this information when citing this paper.

Elementary Structural Motifs in a Random Network of Cytosine Adsorbed on a Gold(111) Surface

Roberto Otero,^{1*} Maya Lukas,^{1†} Ross E. A. Kelly,^{2‡} Wei Xu,¹ Erik Lægsgaard,¹ Ivan Stensgaard,¹ Lev N. Kantorovich,² Flemming Besenbacher^{1§}

Nonsymmetrical organic molecules adsorbed on solid surfaces may assemble into random networks, thereby providing model systems for organic glasses that can be directly observed by scanning tunneling microscopy (STM). We investigated the structure of a disordered cytosine network on a gold(111) surface created by thermal quenching, to temperatures below 150 K, of the two-dimensional fluid present on the surface at room temperature. Comparison of STM images to density functional theory calculations allowed us to identify three elementary structural motifs (zigzag filaments and five- and six-membered rings) that underlie the whole supramolecular random network. The identification of elementary structural motifs may provide a new framework for understanding medium-range order in amorphous and glassy systems.

The microscopic description of glasses and amorphous solids is in general very challenging because of the lack of long-range order in their structure (*1*). The structure of amorphous solids has traditionally been studied by space-averaging diffraction techniques, which have provided a detailed description of such materials on the macroscopic scale (*1, 2*). However, much less is known about the local structure of such disordered solids. Important breakthroughs in this respect came from optical microscopy studies of colloidal glasses (*3, 4*). However, because of the nonscalable behavior of the

energy-relaxation processes with particle size, many details of how the molecular glasses persist and the dynamics of the glass transition cannot be answered with these model systems (*4*).

Some organic molecules can form hydrogen bonds via peripheral functional groups that may be distributed in a highly anisotropic way. Such molecules have the potential to organize in random arrangements when deposited on atomically flat solid surfaces. The structure and dynamics of these systems can be addressed by scanning probe techniques at the molecular level (*5–7*), provided the adsorption geometry is planar; they thereby have the potential to become a model system for studies on the structure of amorphous solids. In principle, the realization of such disordered systems also requires molecule-surface interactions to be much weaker than molecule-molecule interactions: If the molecules had an ability to arrange themselves in the gas phase in planar disordered structures, a strong interaction of the molecules with the surface would force them to form well-ordered structures controlled by the surface periodicity.

The formation of a planar network is exemplified by the case of guanine (G) on Au(111) (*8*). In this case, G self-assembles into a network of G quartets, as determined almost entirely by

hydrogen bonding between the adsorbates; the role of the surface is only that of promoting planarity, as the corrugation of the potential energy surface is rather flat. However, the symmetry of the functional groups around the G molecules enables ordered networks to be formed.

We have studied the molecular-scale self-assembly of a cytosine (C) network on the Au(111) surface in real space by means of scanning tunneling microscopy (STM). In this case, a supramolecular network also forms, but unlike the previously reported case of a G structure, the C network lacks long-range order. DNA base molecules adsorb weakly on noble metal surfaces, with an adsorption potential energy surface displaying a small corrugation and a weak charge transfer between molecule and substrate (*8–11*). Experimentally we find that the C molecules are sufficiently mobile on the Au(111) surface, so that the molecular layer can be considered as a two-dimensional (2D) fluid at room temperature. Previous theoretical studies indicate that because of the large number of hydrogen-bond donor and acceptor groups with which C is provided, a relatively large number of stable C-C dimer configurations could form, involving double hydrogen bonds between groups of neighboring peripheral functionalities (or “binding sites”; see inset in Fig. 1A) (*12*). The multiplicity of the strongest C-C dimer states with similar binding energies and the nonsymmetrical distribution of the corresponding binding sites over the periphery of the molecules suggest that intermolecular interactions alone might direct the growth of disordered structures. Indeed, our STM results reveal that the 2D fluid of mobile C molecules found at room temperature, when quenched to low temperatures at a cooling rate of about 20 K/min on average, assembles into disordered structures, thus behaving like a 2D glass.

When C molecules at a coverage of less than one monolayer (ML) are deposited on Au(111) at room temperature and the sample is imaged by STM at temperatures of ≥ 180 K, no individual C molecules are observed because of their high mobility. Instead, noise is observed in the STM signal, the origin of which is associated with mobile C molecules diffusing under the STM tip much faster than the average STM scanning

¹Interdisciplinary Nanoscience Center, Centre for DNA Nanotechnology, and Department of Physics and Astronomy, University of Aarhus, 8000 Aarhus C, Denmark. ²Department of Physics, School of Physical Sciences and Engineering, King's College London, Strand, London WC2R 2LS, UK.

*Present address: Departamento de Física de la Materia Condensada, Facultad de Ciencias, Universidad Autónoma de Madrid, and Instituto Madrileño de Estudios Avanzados en Nanociencia, 28049 Madrid, Spain.

†Present address: Institute for Nanotechnology, Forschungszentrum Karlsruhe, Postfach 3640, D-76021 Karlsruhe, Germany.

‡Present address: Department of Physics and Astronomy, University College London, Gower Street, London WC1E 6BT, UK.

§To whom correspondence should be addressed. E-mail: fbe@inano.dk

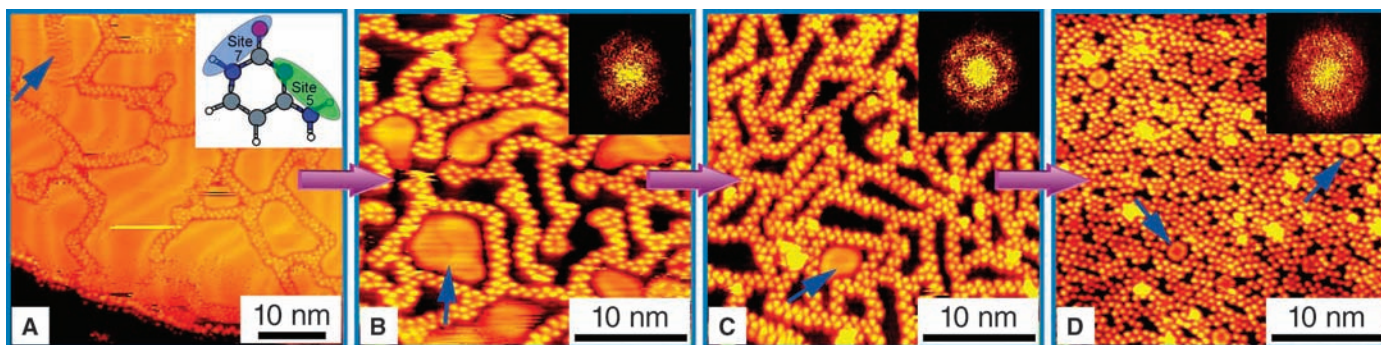


Fig. 1. STM images of cytosine structures with increasing surface coverage (as denoted by the pink arrows). (A to C) Blue arrows indicate mobile C zigzag branches (A) and C molecules or clusters trapped in nanocages that appear as blurs [(B) and (C)]. The inset of (A) shows the most important binding sites used to form

double hydrogen bonds between cytosine molecules. (D) At higher coverages, the blurs show internal structures as 5- or 6-fold rings. Scanning conditions: (A), tunneling current $I_t = -0.5$ nA, tunneling voltage $V_t = -1767$ mV; (B), $I_t = -0.3$ nA, $V_t = -1767$ mV; (C), $I_t = -0.7$ nA, $V_t = -1250$ mV; (D), $I_t = -0.2$ nA, $V_t = -1250$ mV.

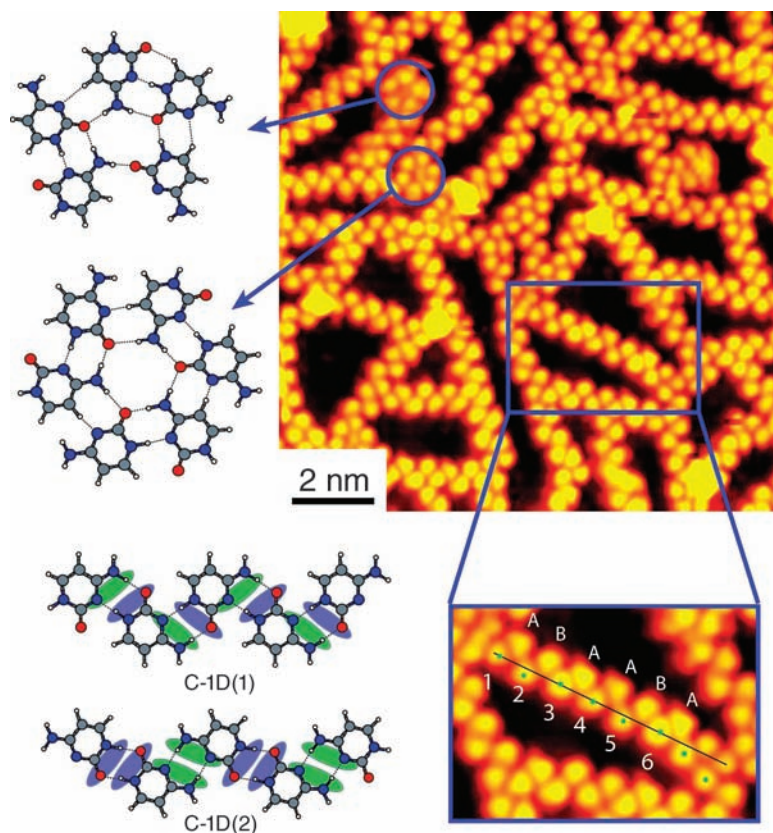


Fig. 2. Three elementary structural motifs (filaments, 5- and 6-fold rings) are compared with the theoretical models. The color coding in the filament models (see inset of Fig. 1A) indicates the binding sites 5 and 7 involved in the two filaments, which makes the chirality of the molecules easier to recognize. The enlarged image shows that the seemingly straight filaments have no translational periodicity. The noncircular shapes of the molecules, which are clearly not tip artifacts (molecules A are mirror images of B), can be recognized in the high-resolution STM images. A line connecting the centers (indicated by green dots) of molecules 1 and 6 is used as a reference. Molecules 1, 3, 4, and 6 binding to molecules A are centered along the reference line, whereas molecules 2 and 5 binding to molecules B are off the reference line. Thus, the above evidence strongly suggests that the dimers 1-A, 3-A, 4-A, and 6-A should be different from dimers 2-B and 5-B, indicating that the filament changes its structure after two or three dimers. Scanning conditions: $I_t = -0.7$ nA, $V_t = -1250$ mV.

time (13, 14). We refer to this state as a 2D fluid. A series of STM images recorded at low temperatures (120 to 150 K) for increasing coverages on the surface is shown in Fig. 1. Near 1 ML, the observed C structure is clearly disordered (Fig. 1D) with no long-range periodicity,

and the C structure thus represents an amorphous 2D system. This long-range disorder is reflected in its fast Fourier transform (FFT), shown in the inset of Fig. 1D, which reveals only a bright rim corresponding roughly to a constant first-neighbors distance. This short-range order is

characteristic of most covalent and metallic glasses, thus indicating that the amorphous structure depicted in Fig. 1D can be described as a 2D glass.

The lack of long-range order is also apparent at lower C coverages (Fig. 1, A to C), although a slight anisotropy in the intensity distribution of the FFT of the STM images along the high-symmetry directions of the gold substrate seems to indicate a small but measurable templating effect of the substrate on the molecular arrangement. For low C coverages (below 0.5 ML), the diffusion dynamics of the C molecules and supra-molecular clusters is revealed even at 100 K. Time-lapse STM movies recorded with the fast-scanning Aarhus STM reveal rearrangements of the different structural elements with respect to each other (see movie S1). Some of the C structures appear as blurred protrusions in the STM images and cannot be resolved into their molecular constituents. In Fig. 1, B to D, these blurred protrusions can be found in the “nanocages” between randomly oriented C filaments. Movie S2 shows that the C-related protrusions may move in and out of a “nanocage” if manipulation with the STM tip breaks one of its “walls.” Upon subsequent increase of the C coverage, the number of blurred protrusions decreases, and these initially featureless blurred protrusions (see Fig. 1B, where one example is indicated by blue arrow) begin to display some internal structure, first appearing like a “doughnut” (Fig. 1C, blue arrow) and subsequently like blurred 5- and 6-fold rings (Fig. 1D, blue arrows). These findings suggest that the blurred structures correspond to mobile C molecules or clusters enclosed in the “nanocages” of the random C network, unable to attach to it.

A detailed analysis of the STM images obtained for coverages below 1 ML revealed that every C molecule belongs to at least one of the following three structural units: (i) zigzag filaments, (ii) 5-fold rings, and (iii) 6-fold rings (Fig. 2). More than 200 images were analyzed for more than five different coverages, and for each coverage at least 20 images were examined. Thus, for our model system, the problem of describing this disordered structure can be reduced to the

much simpler problem of understanding how these three elementary structural motifs link together.

To further characterize the structure of the random C network, we performed *ab initio* density functional theory (DFT) calculations. The minimum-energy configurations for C molecules with geometries similar to the zigzag chains and the 5- and 6-fold rings revealed in the STM images are shown in Fig. 2. By systematically attaching molecules to each other in all possible ways (12), several configurations with very similar binding energies were found for all three structures. The two most stable models for the periodic zigzag filaments, obtained by assuming that the unit cell is composed of two C molecules (that is, a C-C dimer), are denoted C-1D(1) and C-1D(2), respectively. The calculated binding energies of about 0.9 eV/molecule for these two structures are very similar and are much larger than those obtained for 5- and 6-fold C rings (0.6 eV/molecule), in good agreement with the experimental finding that the filaments are the most common structure observed in the STM images. Because the stabilization energies of the two filamentary structures C-1D(1) and C-1D(2) corresponding to the same motif are very similar, we assume that all of them coexist in the random cytosine network, and their very similar geometry makes them indistinguishable by STM. From the calculations we find that the interaction with the gold surface is much weaker (adsorption energy found to be 0.1 eV) than the identified intermolecular hydrogen bonding strength between the C molecules. Although there is a weak indication in the FFT images of a preferential alignment of the filaments along the symmetry directions of the gold surface (Fig. 1C), this effect is much smaller than that of the hydrogen bonding that drives the assembly of C molecules.

We next addressed how these different elementary structural motifs interconnect with each other to form the specific disordered cytosine networks. The ends of the two stable finite filament segments (Fig. 2) exhibit a number of exposed hydrogen-bonding groups—that is, they are “sticky”—whereas the peripheral functional groups exposed on the sides of the filaments are mostly nonpolar and thus are less prone to form stable bonds to neighboring C molecules. Correspondingly, we never observed a “bare” filament termination. As shown in Fig. 3, A and C, the filaments are always linked to some other filament through a 6-fold ring or in a T-junction fashion (possible models for which are displayed in Fig. 3, B, D, and E). Similarly, the “sticky ends” of any two filaments can join head-to-tail, resulting in either bent or apparently linear filament structures (Fig. 3, F and G). Our STM images show that indeed most of the observed filaments that are longer than four to six dimers quite often are bent (Fig. 3C). Furthermore, our high-resolution STM images reveal a change in the shape of molecules (marked as A and B in the enlarged STM image in Fig. 2) along straight filaments in positions that would be equivalent if

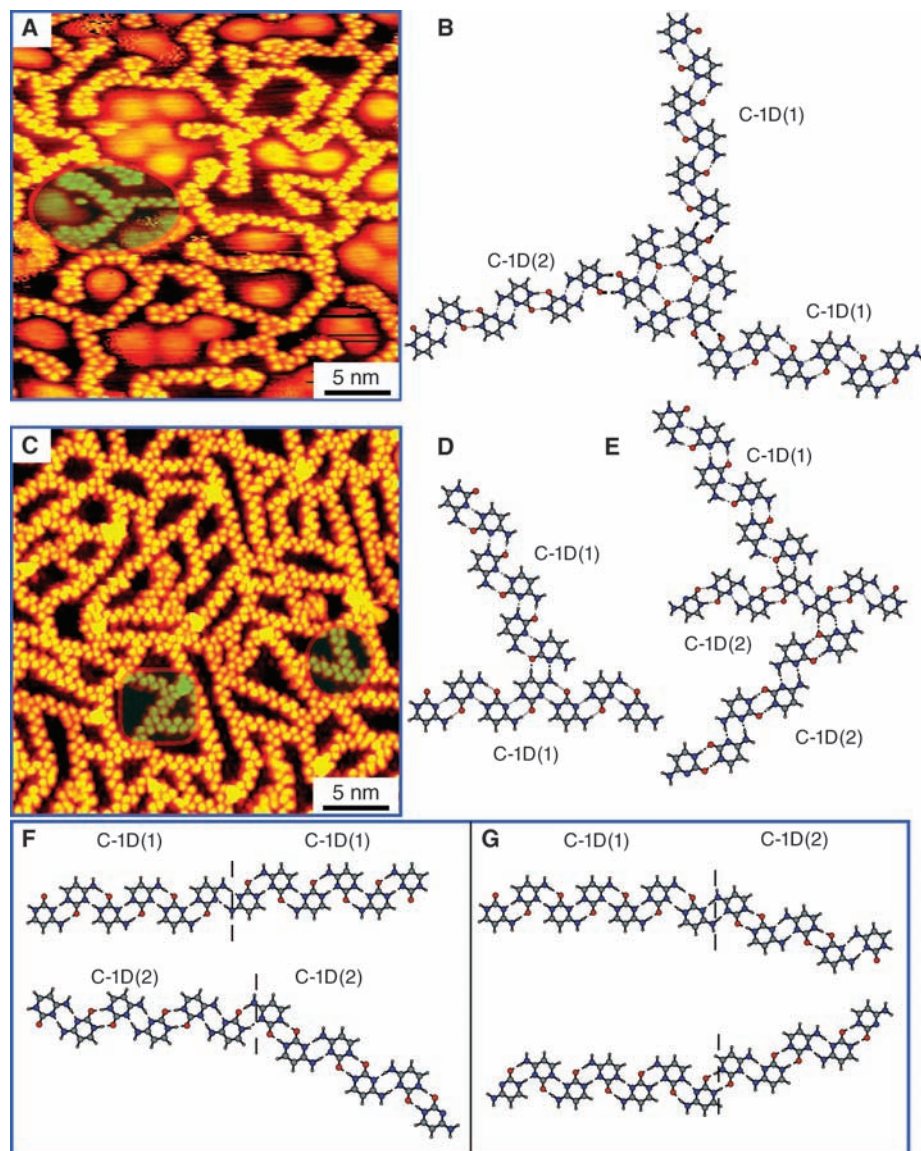


Fig. 3. (A and B) An STM image (A) and a theoretically predicted structure (B) show the connections between C filaments and 6-fold rings in a “roundabout” fashion. (C) An STM image shows the C filaments linked together mainly via T- and bending junctions. (D to G) The corresponding theoretically predicted structures. Examples of “roundabout” and T-junction motifs are highlighted by a red oval in (A) and a red square in (C). Scanning conditions: (A), $I_t = -0.4$ nA, $V_t = -1051$ mV; (C), $I_t = -0.7$ nA, $V_t = -1250$ mV.

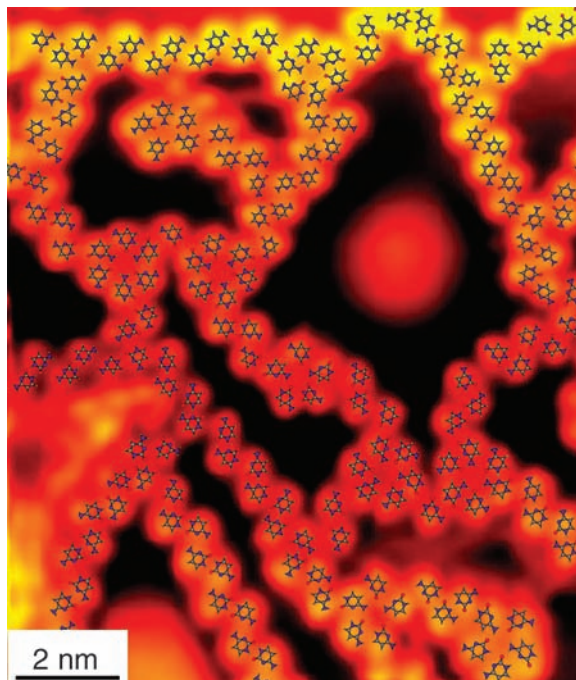
there were translational periodicity. This indicates that these A and B molecules do not have the same orientation; thus, translational periodicity appears only over two to three dimer distances along the filaments.

Figures 3A and 3B depict experimentally and theoretically, respectively, how the “sticky ends” of cytosine filaments can link together through the 6-fold ring in a “roundabout” fashion. As in the case of 5- and 6-fold ring formations, the bonds involved in the interconnections among the different elementary structural motifs will be weaker than those involved in the stabilization of the C-1D structures. On the other hand, the “nonsticky” nature of the filament’s side borders makes it difficult for molecules or molecular clusters trapped inside “nanocages” to attach to

their “walls,” and thus they diffuse fast in the enclosed regions (they appear as blurred protrusions in the STM images discussed above). Thus, by connecting and combining the three elementary structural motifs in the fairly small number of ways just described, the C structures observed in the STM images can be explicitly characterized; an example of this is shown in Fig. 4.

Previous STM experiments performed in an electrochemical environment (15) reveal that another structure for the C-Au(111) system exists in which ordered arrays of zigzag filaments of C molecules lie parallel to each other, bound by weak van der Waals (vdW) forces acting between nonpolar (nonsticky) areas of the filaments. Note that in this arrangement, each molecule is also hydrogen-bonded to two other molecules along

Fig. 4. STM image of a “glassy state” of cytosine on Au(111), with an overlay illustrating that a few elementary hydrogen-bonded structural motifs and their possible connections explain the image. Scanning conditions: $I_t = -0.15$ nA, $V_t = -1767$ mV.



the filament, but it also interacts with two molecules of the neighboring filaments through vdW interactions. In the random network we observed, only hydrogen bonding is involved and the majority of the C molecules are bound to only two neighbors through hydrogen bonding. Hence, because of an additional vdW interaction, the binding energy per molecule in relatively large islands of parallel C filaments will be greater than in a random network containing the same number of molecules. This ensures that the ordered arrangement has the lowest energy, and thus it serves as the 2D cytosine ground state.

Because crystalline islands can only survive if they are larger than some critical size, kinetically their formation is highly unlikely. Indeed, upon fast cooling, the formation rate of a large stable crystalline nucleus cannot compete with the formation rate of much smaller structures such as 5- and 6-fold rings, roundabouts, and T junctions—which are energetically the most stable clusters containing small numbers of C molecules—and the system gets trapped in a random network during the first stage of the kinetic process of assembly formation. Thus, this kinetic process leads to a dynamical capture of the 2D fluid upon fast cooling when the available thermal energy in the system becomes insufficient to facilitate escape from the local order of the liquid state into the ground crystalline state.

We thus conclude that, despite the lack of periodicity in the random cytosine network, we have revealed that only a few elementary structural motifs exist through which C molecules bind to each other, and yet very complex structures can be formed from these structural building blocks. The present cytosine model system is kinetically trapped in a disordered state, much like glass is trapped in the amorphous state, because it would need to

overcome prohibitively large energy barriers to move away from it. Examples of glass-forming systems where the constituents are molecules that can form hydrogen bonds in one of their ends but interact only weakly through their other parts (e.g., ethanol) are known in the literature (16). Our results may reveal an interesting route for studying the structure of organic glasses: performing a systematic search of particularly stable motifs and their possible interconnections.

The structure we describe here is similar to a continuous random network, where the constituents of the network are not individual atoms or molecules but instead consist of a small number of supramolecular elementary motifs, some of

which present medium-range order. The identification of such structural motifs would not have been possible without the proper choice of a model system and the use of STM to reveal the nanoscale order.

References and Notes

1. R. Zallen, *The Physics of Amorphous Solids* (Wiley-VCH, Weinheim, Germany, ed. 1, 2004).
2. S. C. Moss, J. F. Graczyk, *Phys. Rev. Lett.* **23**, 1167 (1969).
3. A. van Blaaderen, P. Wiltzius, *Science* **270**, 1177 (1995).
4. E. R. Weeks, J. C. Crocker, A. C. Levitt, A. Schofield, D. A. Weitz, *Science* **287**, 627 (2000).
5. J. V. Barth, *Annu. Rev. Phys. Chem.* **58**, 375 (2007).
6. F. Rosei *et al.*, *Prog. Surf. Sci.* **71**, 95 (2003).
7. R. Otero, F. Rosei, F. Besenbacher, *Annu. Rev. Phys. Chem.* **57**, 497 (2006).
8. R. Otero *et al.*, *Angew. Chem. Int. Ed.* **44**, 2270 (2005).
9. M. Furukawa, H. Tanaka, T. Kawai, *J. Chem. Phys.* **115**, 3419 (2001).
10. Q. Chen, N. V. Richardson, *Nat. Mater.* **2**, 324 (2003).
11. L. M. A. Perdigo *et al.*, *Phys. Rev. B* **73**, 195423 (2006).
12. R. E. A. Kelly, Y. J. Lee, L. N. Kantorovich, *J. Phys. Chem. B* **109**, 22045 (2005).
13. M. Schunack *et al.*, *Phys. Rev. Lett.* **86**, 456 (2001).
14. M. Schunack *et al.*, *Phys. Rev. Lett.* **88**, 156102 (2002).
15. N. J. Tao, J. A. DeRose, S. M. Lindsay, *J. Phys. Chem.* **97**, 910 (1993).
16. M. A. Ramos *et al.*, *Phys. Rev. Lett.* **78**, 82 (1997).
17. Supported by an EU individual Marie Curie Fellowship, EU-RTN project Atomic and Molecular Manipulation as a New Tool for Science and Technology, and EU project Picolnside (R.O. and M.L.), and by the Danish Ministry for Science, Technology and Innovation through the iNANO Center, the Danish Research Councils, the Danish National Research Foundation, the Carlsberg Foundation, and UK Engineering and Physical Sciences Research Council grant GR/P01427/01. We thank the Materials Chemistry Consortium for computer time on the HPCx supercomputer.

Supporting Online Material

www.sciencemag.org/cgi/content/full/1150532/DC1

Materials and Methods

References

Movies S1 and S2

14 September 2007; accepted 4 December 2007

Published online 13 December 2007;

10.1126/science.1150532

Include this information when citing this paper.

The Subduction Zone Flow Field from Seismic Anisotropy: A Global View

Maureen D. Long* and Paul G. Silver

Although the morphologies of subducting slabs have been relatively well characterized, the character of the mantle flow field that accompanies subduction remains poorly understood. To analyze this pattern of flow, we compiled observations of seismic anisotropy, as manifested by shear wave splitting. Data from 13 subduction zones reveal systematic variations in both mantle-wedge and slab anisotropy with the magnitude of trench migration velocity $|V_t|$. These variations can be explained by flow along the strike of the trench induced by trench motion. This flow dominates beneath the slab, where its magnitude scales with $|V_t|$. In the mantle wedge, this flow interacts with classical corner flow produced by the convergence velocity V_c ; their relative influence is governed by the relative magnitude of $|V_t|$ and V_c .

Upon propagation through an anisotropic medium, a shear wave is split into two orthogonally polarized components and accumulates a delay time, δt , between the fast and slow waves; the fast direction, ϕ , and δt are

measured (1, 2). In the upper mantle, anisotropy results from the strain-induced lattice preferred orientation (LPO) of olivine (3–6), so that if the relationship between deformation and LPO is known or inferred, shear wave splitting measure-